Journal of Engineering and Sustainable Development
Vol. 28, No. 06, November 2024
https://jeasd.uomustansiriyah.edu.iq/index.php/jeasd
ISSN 2520-0917
Research Article
https://doi.org/10.31272/jeasd.28.6.1

Numerical Study of Double-Diffusive Mixed Convection Flow in Channel with Hybrid Nanofluid in Porous Medium

Karrar Kadhim Jaber[1], Khaled Al-Farhany[2*], Dhafer A. Hamzah[3], Wael Al-Kouz[4]

[1,2,3] Department of Mechanical Engineering, College of Engineering, University of Al-Qadisiyah, Al-Qadisiyah, 58001, Iraq
[4] Department of Engineering and Industrial Professions, College of Engineering, University of North Alabama, Florence, Al, 35632, USA

[1] https://orcid.org/0009-0000-4907-4826
[2] https://orcid.org/0000-0002-5806-3800
[3] https://orcid.org/0000-0002-9790-4676
[4] https://orcid.org/0000-0002-2116-7673
[*]Email: khaled.alfarhany@qu.edu.iq

Article Info

Received	18/07/2024
Revised	23/09/2024
Accepted	12/10/2024

Abstract

The main objective of this work is to investigate numerically double-diffusive mixed convection flow in a channel filled with a hybrid nanofluid of Cu-Al_2O_3 in a porous media. It is considered that the cavity's left wall is continuously heated. The fluid flow enters the channel at low concentration and temperature. This work has been looked into two cases: Case 1, where it is supposed that the left wall cavity has high concentrations, and Case 2, where it is expected that the right wall cavity has high concentrations. The cavity's remaining walls are impermeable and thermally insulated. Non-dimension governing equations are solved with the finite element method. Parameters effects of Reynolds number($10 \le Re \le 100$), Richardson number ($2 \le Ri \le 10$), Darcy number ($Da=10^{-2},10^{-4}$), Lewis number ($1 \le Le \le 5$), buoyancy ratio, N=1, the solid volume fraction ($\phi=0.02$), and Prandtl number (Pr=6.2). The results show that increasing Reynolds, Richardson, and Darcy numbers increases the average Nusselt while it decreases by increasing Lewis number. In addition, Sherwood numbers increase with increasing Reynolds, Lewis, and Darcy numbers while they decrease with Richardson numbers for both cases. When the Reynolds number increases from 10 to 50 at ($Da=10^{-4}$) and (Ri =10), the Nusselt number increases by 102%, while the Sherwood number decreases to 72%.

Keywords: Computational Fluid Dynamics CFD: Double diffusion: Hybrid nanofluid; Mixed convection; Open channel; Porous medium

1. Introduction

Several researchers have conducted extensive analyses utilizing both experimental and numerical techniques in natural, forced, and mixed convection. Fluid flow patterns have garnered significant interest in terms of understanding, forecasting, and work. From then on, substantial research was done on fluid dynamics. This phenomenon is essential in science and engineering systems due to the numerous uses of mixed or combined convection and heat transfer of fluid flow into cavities, such as high-performance insulation in buildings, heat exchangers, drying technologies, ventilation systems, and solar panels [1]. One of the fields with the most significant amount of research is mixed convection flows in cavities, aiming to gain quantitative knowledge and expand practical applications [2],[3].

Identifying fluid flow and heat transfer parameters under various Richardson numbers was the primary goal of the authors' work. For values of Ri less than 0.1, forced convection is the dominant mode. Natural convection occurs when Ri is greater than 10, while mixed convection occurs when Ri is between 0.1 and 10 Zafar and Alam [4]. The literature has numerous investigations of mixed convection in a horizontal channel using Cu-Al_2O_3 hybrid nanofluid in a porous medium to comprehend the intricate physical processes involved in fluid flow and heat transfer. Sabbar et al. [5] studied the effects of mixed convection on the fluid-structure interaction in the channel. The bottom of the hollow was equipped with a permanent heat source, and the other walls were built adiabatically. Elsaid and Abdel-Wahed [6] studied the mixed convection of a hybrid nanofluid (H_2O–Cu/Al_2O_3) moving

through a vertical channel. The problem was converted into ordinary differential equations and solved analytically for both buoyancy cases using a dimensionless variable technique. Jahanshaloo et al. [7] investigated the alumina-water nanofluid flow's heat transfer characteristics and performance in a channel with a heated cavity. The effects of changes in the Grashof number in different aspect ratios of cavities and volume fractions of nanoparticles and the characteristics and efficiency of heat transmission were considered. Ruhani et al. [8] examined the effects of temperature and the volume percentage of nanoparticles on the viscosity of a hybrid nanofluid. (50%Ag/50%ZnO)/water. offered a model for calculating the dynamic viscosity of a hybrid nanofluid. It was discovered that when temperatures increase, the dynamic viscosity decreases while the nanoparticle fraction rises. Furthermore, at all temperatures, the relative viscosity of nanofluids increases in lockstep with the volume fraction of nanoparticles. Raisi et al. [9] examined the mixed convection heat transfer of a Cu-water nanofluid in a parallel-plate vertical channel when placed under a magnetic field. The outcomes displayed various magnetic field effects on the average Nusselt number observed for different Richardson numbers. The average Nusselt number for the Richardson numbers Ri = 1 and Ri = 100 was independent of the Hartmann number. The average Nusselt number increases for low Richardson numbers in proportion to the solid volume fraction. As the Richardson number increases, the solid volume percentage has less effect. Manay et al.[10] analyzed the characteristics of the mixed convection heat transfer caused by nanofluid flow in a circular microchannel. The particle volume ratio (0, 0.25, and 0.75%) and Reynolds number (200–60) effects on heat transfer by mixed convection were investigated for both assisting and opposing flow circumstances. Sindhu et al. [11] simulated a microchannel heat sink for cooling Cu:γ−ALOOH/Water. The microchannel heat sink was simulated using the extended two-equation model for the energy equation and the Darcy model for the momentum equation in accordance with the porous media approach. The results indicate that when the volume percentage of nanoparticles in the hybrid mixes increased, the temperature of both solid surfaces and hybrid nanofluids fell. Increasing the volume percentage of nanoparticles in the hybrid mixture causes improved Brownian movement, which distributes heat to the surrounding area. This results in an increase in the rate of heat transmission. The thermal field for the solid section and Cu: γ − ALOOH/Water increases with increasing Darcy number. Al-Farhany et al.[12] researched the characteristics of fluid flow and heat transfer in a horizontal rectangular channel with an elliptical obstacle and an open trapezoidal enclosure using (Cu-water) nanofluid under magnetohydrodynamic influences. Qureshi et al. [13] studied a hybrid nanofluid's flow and heat transfer characteristics in a horizontal channel with a cavity that holds an impediment. A stable and higher-order finite element approach based on Galerkin was applied for various physical parameters to model the dimensionless governing partial equations. Gumir et al. [14] employed a hybrid (35%MWCNT-65%Fe_3O_4)/water nanofluid to investigate the natural convection numerically in a two-dimensional enclosure with a finite solid wavy wall. The Darcy-Brinkman-Forchheimer model can represent a porous medium with a hybrid nanofluid. The investigation employed the following dimensionless parameters: modified Rayleigh number ($Ra^*= 10^2$, 10^3, 10^4, and 10^6), Darcy number ($Da= 10^{-2}$, 10^{-4} and 10^{-6}), Solid volume fraction (ϕ= 0.01, 0.03, and 0.05), undulation number (N= 1, 3, 5, and 7), amplitude of the wavy wall (A= 0.1, 0.2, and 0.3), and Prandtl number = 7.2 at constant high porosity. As the ϕ increases, the stream function decreases due to the increased dynamic viscosity of the fluid caused by the addition of nanoparticles. The average Nusselt number increases with nanoparticle concentration and is reliant on it. Raising the Ra* enhances the buoyant force and natural convection effect, increasing the stream function. Al-Farhany et al. [15] researched, using numerical methods, the effects of MHD on mixed convection in an open channel heated by the bottom wall, applying the finite element technique approach. The lowest wall was partially heated, while the other walls were adiabatic, and the air entering the channel was cold. Al-Farhany et al. [16] investigated how MHD affected the mixed convection of a Cu-water nanofluid in a horizontal channel that was coupled to two open enclosures that held a porous material. In order to solve the investigated equations, the finite element approach has been applied. Buonomo et al. [17] examined mixing convection in the air inside a heated channel that had aluminum foam only partially inside of it. Experimental research was conducted on two wall heat flux values and Reynolds numbers ranging from 100 to 300. Foams with higher pore per inch values have lower average wall temperature values, even though the local wall temperatures behaved differently for each value. The foam in the heated channel results in lower secondary motions compared to the clean instances. When the foam is in the heated channel, the average Nusselt number increases, and the foam's influence seems to be more pronounced for higher Reynolds number values. Barletta and Rees [18] examined the convective flow over a horizontal porous duct. Uniform and symmetric heat fluxes were applied to the upper and bottom impermeable limits. The Darcy-Forchheimer law has been applied to simulate the flow in the porous media by considering the influence of form-drag. The investigation of a two-dimensional, steady, incompressible mixed convection flow in a cavity-filled channel has been examined. Utilizing the Darcy-Brinkman-Forchheimer approach, a saturated porous medium is used to populate the cavity with a Cu-Al2O3 hybrid nanofluid. Nath and Krishnan [19] investigated using a Cu-water nanofluid in a backward-facing channel for mixed convective heat and mass transfer. Galerkin's weighted residual finite element method has been used to solve the governing equations to obtain the field variables. Abd Al-Hassan and Ismael [20] investigated the unstable mixed convection of double diffusion in an open cavity compound connected to a horizontal channel. The governing equations were solved using a finite element approach.Throughout the investigation, the following parameters were constant: the buoyancy ratio, N = 0.5; the Lewis number, Le = 20; the Darcy number, $Da = 10^{-3}$; and the Prandtl number, Pr = 6.26. Reynolds number (Re = 50–250), Richardson number (Ri = 0.01–100), and porous layer thickness (Hp = 0.25–1) were the controlling factors. The outcomes demonstrated that the opposite scenario supplies the largest convective heat transfer. The percentage gains for the opposing and aiding cases at Re = 50 and 250 were 53.07 and 90.18% for Ri = 0.01 and 36.30 and 17.81% for Ri = 100. Al-Farhany and

Turan [21] investigated the mass and heat transfer process using double-diffusive natural convection in a rectangular chamber that was filled with a porous substance and inclined. A finite volume approach has been applied to solve the non-dimensional governing equations, and the SIMPLER technique has been used to address the pressure-velocity coupling. The results revealed that although the average Sherwood and Nusselt numbers declined as the aspect ratio increased, the opposite was true for the inclined angle. Regarding the buoyancy ratio impact, the Nusselt number rises for ($N \geq -1$) and falls for ($N \leq -1$). This was also the Sherwood number's behavior. Furthermore, as late extended their job, the Lewis number increased, causing the Sherwood number to rise and the Nusselt number to decrease [22].

This issue has practical implications for many technical applications, including heat exchangers and solar collectors; further research is required to advance knowledge. This work aims to investigate the mixed convective heat and mass transfer in a cavity saturated with Cu-Al_2O_3 hybrid nanofluid in a porous medium in a channel. The problem still needs to be considered or looked into, according to the authors' knowledge and the literature survey of this work. The fluid entered the channel at a low concentration (C_l) and constant cold temperature (T_C), with the left wall of the hollow assumed to be at constant temperature (T_h). This work considered two cases, depending on the high concentration (C_h) positions. The cavity's remaining walls are insulated from heat. A finite element pair Q_2/P_1^{disc} results in the L2-norm's third- and second-order precision for pressure and velocity/temperature, respectively. The influence of Reynolds number (Re), Richardson number (Ri), Darcy number (Da), and Lewis number (Le) on the mixed convection rate in a channel cavity are the main subjects of this work.

2. Mathematical Modelling

Fig. 1 demonstrates a two-dimensional rectangular chamber connected to the lower part of an open channel. A Cu-Al_2O_3/water hybrid nanofluid is selected to flow through a porous medium over the entire domain. In this work, the channel length is equivalent to 6H, and the channel height is represented by 0.5H. The rectangular chamber width and height are 2H and H, respectively. The porous medium is considered to be saturated with the hybrid nanofluid. Heat equilibrium is assumed between the spherical Cu-Al_2O_3 nanoparticles and the pure fluid (water). There is consistent low temperature (T_C) and concentration (C_l) flow through the left side of the channel, while the left side of the wall has homogenous heat at Th. This work looked into two cases: Case 1, where it was supposed that the left wall cavity had high concentrations (C_h), and Case 2, where it was thought that the right wall cavity had high concentrations (C_h). The cavity's remaining walls are impermeable and thermally insulated. Uniformity in size and shape characterizes solid particles. With a Prandtl value of 6.2, water is the fluid under consideration. The solid porous matrix's thermal conductivity is assumed to be 205 W/mK, while the porous layer's porosity is fixed at $\varepsilon = 0.7$, and the solid volume fraction is used as ($\phi_{Cu} = \phi_{Al2O3} = 0.01$). Table 1 lists the base fluids and the nanoparticles' constant thermo-physical characteristics.

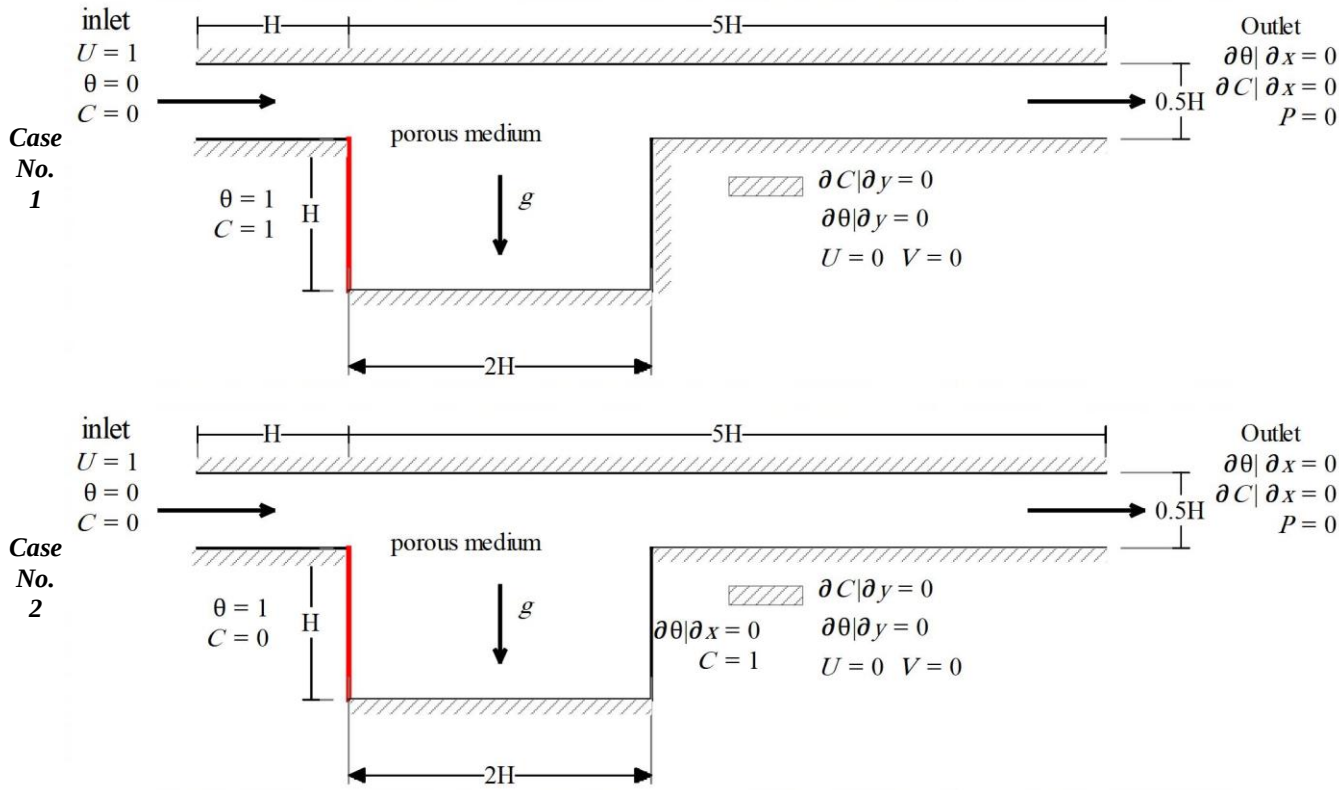

Figure 1. The geometry of research work.

Table 1. Thermophysical characteristics of the hybrid nanofluid constituents [23]

Property	Water	Copper (Cu)	Alumina (Al_2O_3)
ρ (kg/m^3)	997.1	8933	3970
Cp(J/kg K)	4179	385	765
k(W/m K)	0.613	401	40
β(1/K)	21×10^{-5}	1.67×10^{-5}	0.85×10^{-5}

2.1. Equations of Conservation

The conservation equations are the non-dimensional governing equations of continuity, motion, and energy. [20], [24], [25]:

$$\frac{\partial U}{\partial X}+\frac{\partial V}{\partial Y}=0 \tag{1}$$

$$\frac{1}{\varepsilon^2}\left(U\frac{\partial U}{\partial X}+V\frac{\partial U}{\partial Y}\right)=-\frac{\partial P}{\partial X}+\frac{1}{\varepsilon\,\mathrm{Re}}\frac{\rho_f}{\rho_{hnf}}\frac{1}{(1-\phi)^{2.5}}\left(\frac{\partial^2 U}{\partial X^2}+\frac{\partial^2 U}{\partial Y^2}\right) \tag{2}$$
$$-\frac{\mu_{hnf}}{\rho_{hnf}\nu_f}\frac{1}{\mathrm{Re}\,Da}U-\frac{1.75}{\sqrt{150Da}\,\varepsilon^{\frac{3}{2}}}\left(\sqrt{U^2+V^2}\right)U$$

$$\frac{1}{\varepsilon^2}\left(U\frac{\partial V}{\partial X}+V\frac{\partial V}{\partial Y}\right)=-\frac{\partial P}{\partial Y}+\frac{1}{\varepsilon\,\mathrm{Re}}\frac{\rho_f}{\rho_{hnf}}\frac{1}{(1-\phi)^{2.5}}\left(\frac{\partial^2 V}{\partial X^2}+\frac{\partial^2 V}{\partial Y^2}\right)$$
$$-\frac{\mu_{hnf}}{\rho_{hnf}\nu_f}\frac{1}{\mathrm{Re}\,Da}V\quad-\frac{1.75}{\sqrt{150Da}\,\varepsilon^{\frac{3}{2}}}\left(\sqrt{U^2+V^2}\right)V$$
$$+Ri\,\frac{\rho_f}{\rho_{hnf}}\left(1-\phi+\left(\frac{\rho_{s1}\beta_{s1}\phi_{s1}+\rho_{s2}\beta_{s2}\phi_{s2}}{\rho_f\beta_f}\right)\right)(\theta+NC)$$

(2)

$$U\frac{\partial\theta}{\partial X}+V\frac{\partial\theta}{\partial Y}=\frac{1}{\mathrm{Re}\,Pr}\frac{\alpha_{hnf}}{\alpha_f}\frac{k_m}{k_{hnf}}\left(\frac{\partial^2\theta}{\partial X^2}+\frac{\partial^2\theta}{\partial Y^2}\right) \tag{3}$$

$$U\frac{\partial C}{\partial X}+V\frac{\partial C}{\partial Y}=\frac{1}{\mathrm{Re}\,\mathrm{Pr}\,Le}\left(\frac{\partial^2 C}{\partial X^2}+\frac{\partial^2 C}{\partial Y^2}\right) \tag{4}$$

2.2. Properties of Hybrid Nanofluid

Density (ρ_{hnf}), a factor of thermal expansion (α_{hnf}), thermal capacitance (cp_{hnf}), and heat diffusivity (β_{hnf}) are the relationships that characterize the efficient physical characteristics of the hybrid nanofluid in the present investigation, which calculated using the following equations are given by [24] :

$$\rho_{hnf}=(1-\phi)\rho_{bf}+\left(\phi_{\mathbf{Al_2O_3}}\cdot\rho_{\mathbf{Al_2O_3}}+\phi_{\mathbf{Cu}}\cdot\rho_{\mathbf{Cu}}\right) \tag{5}$$

$$\alpha_{hnf}=\frac{k_{hnf}}{(\rho cp)_{hnf}} \tag{6}$$

$$(\rho cp)_{hnf}=(1-\phi)(\rho cp)_{bf}+\left(\phi_{\mathbf{Al_2O_3}}\cdot\rho_{\mathbf{Al_2O_3}}\cdot cp_{\mathbf{Al_2O_3}}+\phi_{\mathbf{Cu}}\cdot\rho_{\mathbf{Cu}}\cdot cp_{\mathbf{Cu}}\right) \tag{7}$$

$$(\rho\beta)_{hnf}=(1-\phi)(\rho\beta)_{bf}+\left(\phi_{\mathbf{Al_2O_3}}\cdot\rho_{\mathbf{Al_2O_3}}\cdot\beta_{\mathbf{Al_2O_3}}+\phi_{\mathbf{Cu}}\cdot\rho_{\mathbf{Cu}}\cdot\beta_{\mathbf{Cu}}\right) \tag{8}$$

$$\mu_{static}=\frac{\mu_f}{(1-\phi)^{2.5}} \tag{9}$$

$$k_m=(1-\varepsilon)k_{sp}+\varepsilon k_{hnf} \tag{10}$$

$$\phi=\phi_{\mathbf{Al_2O_3}}+\phi_{\mathbf{Cu}} \tag{11}$$

Non-dimensional parameters in the above equations are used. [25], [26]

$$U=\frac{uH}{\alpha},V=\frac{vH}{\alpha},X=\frac{x}{H},Y=\frac{y}{H},\theta=\frac{T-T_c}{T_h-Tc} \tag{12}$$

The mixed convection, Reynolds number (Re), Richardson number (Ri), and the Grashof number (Gr), which is represented as can all be found using the dimensionless factors:

$$Re=\frac{\rho_f u_\circ H}{\mu_f},Ri=\frac{Gr}{Re^2},Gr=\frac{g\beta_T\left(\mathrm{T_h}-\mathrm{T_c}\right)H^3}{\nu_f{}^2},Pr=\frac{\upsilon_f}{\alpha_f} \tag{13}$$

$$P=\frac{p}{\rho_{hnf}{}^2u_\circ{}^2},\alpha_f=\frac{k_f}{(\rho Cp)_f},Da=\frac{K}{H^2},K=\frac{\varepsilon^3d_p^2}{150(1-\varepsilon)^2} \tag{14}$$

2.3. Boundary Conditions

The boundary conditions related to the issue are provided by

- In the channel's inlet side

  U= 1 , V= 0 , θ = 0, C=0

- On the cavity's left wall
  - for Case 1: U= 0 , V= 0 , θ = 1, C=1
  - for Case 2: U= 0 , V= 0 , θ = 1, $\partial C/\partial X=0$
- On the cavity's right wall
  - for Case 1: U= 0 , V= 0 , $\partial\theta/\partial X=0$, $\partial C/\partial X=0$
  - for Case 2: U= 0 , V= 0 , $\partial\theta/\partial X=0$, C=1
- Considering the remaining adiabatic channel and cavity walls

  $U=V=\partial\theta/\partial Y=\partial C/\partial Y=0$ for a horizontal wall
- In the channel's outlet side

  $\partial U/\partial X=\partial V/\partial Y=\partial\theta/\partial X=\partial C/\partial X=0$

2.4. The Nusselt and Sherwood Numbers

Heat transfer properties are represented by the Nusselt and Sherwood numbers, which are defined as follows [20]:

The Nusselt and Sherwood local numerals on the vertical walls

$$Nu=-\frac{\partial\theta}{\partial x}\Big|_{x=H} \tag{16}$$

For Case 1, $Sh_{av}=-\frac{\partial C}{\partial x}\Big|_{x=H}$ (15)

For Case 2, $Sh_{av}=\frac{\partial C}{\partial x}\Big|_{x=3H}$ (16)

The average Nusselt number at the vertical walls

$$Nu_{avg} = \frac{1}{H}\int_0^H Nu\,dy \quad (17)$$

Sherwood number averages are generally.

$$Sh_{avg} = \frac{1}{H}\int_0^H Sh\,dy \quad (18)$$

3. Numerical solutions

The Galerkin technique of finite elements is utilized to resolve this work's bounds and dimensionless governing formulas. Gaussian elimination is used to solve the linear subproblems, while the Newton approach is applied to the discretized system of nonlinear equations. Fig. 1. shows the cartesian coordinate of a two-dimensional numerical solution region where the triangular mesh was used for this investigation, as shown in Fig. 2. A grid-independent has been used to achieve high-precision results while minimizing computing time, and the grid size sensitivity must be examined. Table 2 illustrates the relationship in the cavity's left vertical wall between the average value of Nusselt and the number of elements at Re = 100, Ri = 1, Da=0.01 and Pr = 6.2. The average Nusselt number calculated using extra-fine mesh sizes (44649) is similar when using excellent mesh sizes (63779). Therefore, the extra fine mesh size has been chosen for every case in this research.

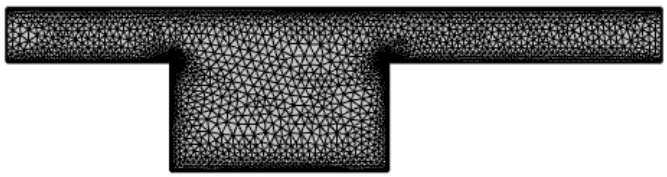

Figure 2. The cavity's triangle mesh distribution

Table 2. The average Nusselt figure and number of elements for Re=100, Ri=1, and Pr = 6.2

Size of Mesh	Elements of Mesh	Average Nusselt Number
Coarse	2713	1.5053
Normal	4079	1.5504
Fine	6643	1.5910
Finer	17435	1.6804
Extra fine	**44649**	**1.7374**
Extremely fine	63779	1.7392

3.1 Validation

This work has been validated in two cases to ensure the results from this code are correct. The first validation can be seen in Fig. 3, which demonstrates the validation of streamline and isotherm in the present work with Kadhim et al.'s [24] work for natural convection using Cu-Al_2O_3/water hybrid nanofluid as a working fluid in the wavy enclosure.

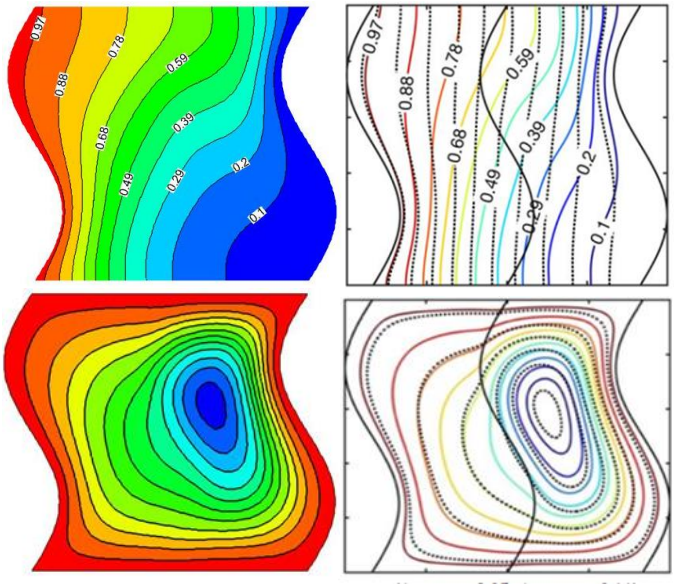

Present work Kadhim et al. [24]

Figure 3. A comparison between the streamline and the isotherms for this work and Kadhim et al. [24] at Ra=10^5,ϕ = 0.2

The results agree with those published by Kadhim et al. [24]. Another numerical comparison with Hussain et al. [25] work at Reynolds number ($Re = 100$), Darcy number ($Da = 10^{-3}$), solid volume fraction ($\phi = 0.04$), inclination angle (γ=0), and Richardson number =1 is shown in Fig. 4. From the figure, it can be seen the result are very closed to the Hussain et al.[25] results.

4. Results and Discussion

The primary goal of this investigation is to investigate the impacts of Cu-Al_2O_3 hybrid nanofluid on the double-diffusion mixed convection heat and mass transfer in a porosity channel. Numerical simulations were carried out for the Reynolds numbers (Re =20,50,80, and 100), Darcy number (Da=0.01 and 0.0001), Richardson number (Ri=2,6, and 10), Lewis number (Le=1,3,5) while the buoyancy ratio equal to (N=1), the solid volume fraction of the hybrid nanofluid (ϕ=0.02), and Prandtl number (Pr=6.2).

For Case 1, Fig. 5 shows how the Reynolds number affects the streamlines, isotherm patterns, and concentration lines. At Re= 20, the initial observations show mild circulation within the cavity and substantial flow along the channel's upper side. Increasing the Reynolds number (up to Re=100) allows a strong flow circulation to fill the cavity almost wholly. In general, as Re increases, the flow strength reaches the center of the cavity. The heat flow from the left vertical can stay in the cavity at low Reynolds numbers. The second column of Fig. 5 shows that when the Re increases, the high isotherms lines get trapped and remain close to the hot wall only due to increased fluid flow velocity, and the channel becomes colder. The flow amplifies as the channel's entrance flow velocity increases, increasing the shear forces. The same behavior can be seen for the concentration; the high concentration variations are near the left wall, as shown in the third column of the concentration lines. A

few variation effects on concentration lines are observed in the second half of the cavity. Increasing the Re will increase the variation of concentration lines along the cavity. It also can be seen that there is a concentration variation in the channel (after the cavity), which increases by increasing the Re because of an increase in the fluid flow with low concentrations.

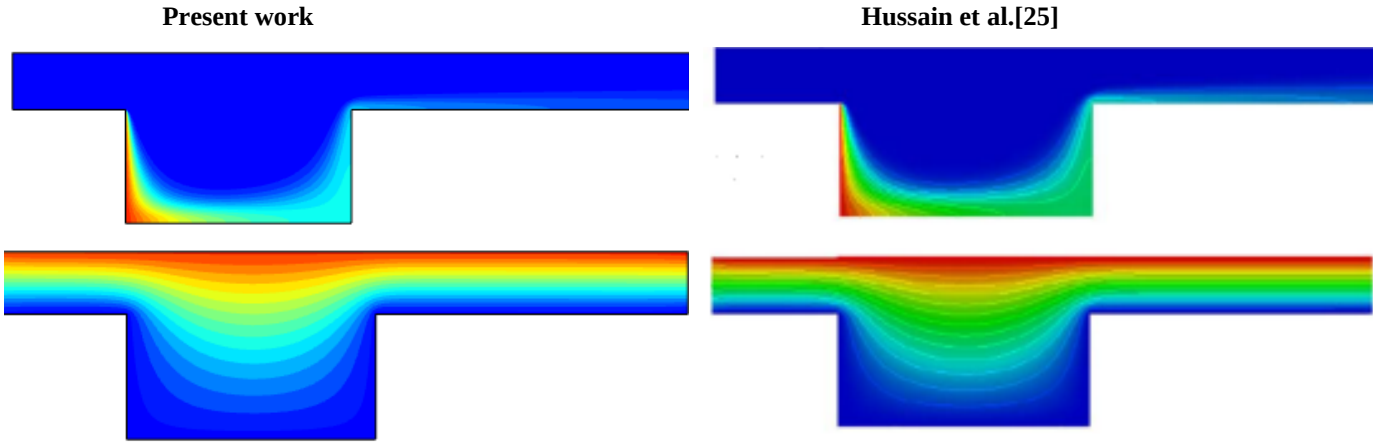

Figure 4. A comparison of the isotherm lines and streamlines for this work and Hussain et al. [25] at Re=100, Ri=1, Da=10-3,γ=0, and ϕ=0.04

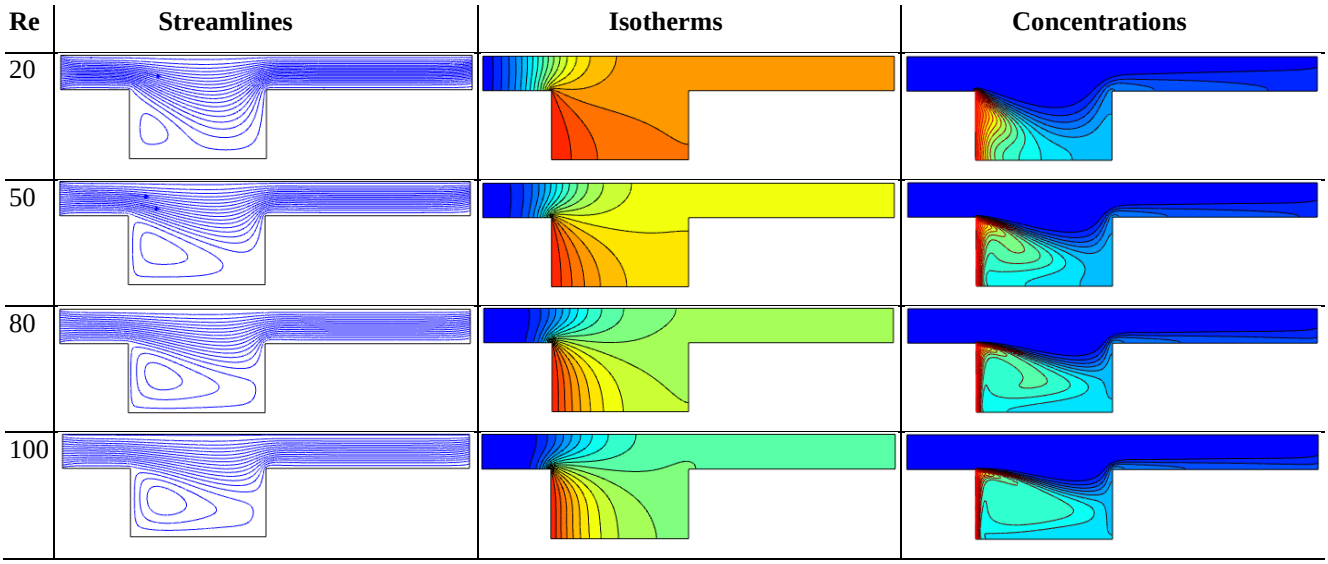

Figure 5. The impact of Reynolds number on streamline, isotherm, and concentrations at Ri=2, Da=10-2, Le=1 for Case1

The same behavior can be seen with increasing the Richardson number on streamlines, isotherms, and concentrations at constant Reynolds numbers, as seen in Fig. 6 for Re = 40, Le=1, and Da = 0.01. In the cavity, the vortices strength increases by increasing Ri due to expanding the boundary force, and the streamlines in the channel above the cavity move almost horizontally due to increasing boundary force. The second column shows that isotherm lines did not change much because of the streamflow on the channel constant (Re=40). An increase in the impact of cold flow and a decrease in heat transmission due to the approaching dominance of mixed convective are observed at the extreme Ri. The same behavior can be seen for concentration.

The influence of Darcy's number on the streamline, isotherms, and concentration lines at Re=20, Le=1, and Ri=6 is portrayed in Fig. 7. There are prominent streamlines on the upper side of the channel. In contrast, the hollow at low permeability shows faint flow patterns. Increasing the Darcy number of objects increases the permeability of the porous layer. As a result, more nanofluids can enter the porous layer, which strengthens the cavity's channel and flow lines. The fluid experiences more fluid resistance via the porous matrix at low Darcy numbers (Da= 10^{-4}), which reduces convective heat transfer. First, the higher-value isotherms are limited to the cavity's left heated wall. Owing to improved permeability, these intense temperature lines spread to the right side of the cavity. As the Darcy number rises to Da= 10^{-2}, the porous material's permeability increases, improving convection and reducing frictional resistance.

Fig. 8 illustrates the impact of the Lewis number on the streamline, isotherm, and concentration lines at Re = 50, Le = 1, Da = 10^{-2}, and Ri = 2. As the Lewis number gauges a fluid's thermal diffusivity rather than its mass diffusivity, a higher value of Le denotes a relatively low mass diffusivity value. The streamlines exhibit near-unity for all values of Le, indicating a modest decrease in fluid flow strength as Le increases. In the vicinity of the heated vertical wall, the solutal boundary layer becomes thinner with increasing Le than the thermal boundary layer. This indicates that the mass transfer rate is also more significant because the thermal resistance is greater than the solutal resistance.

Fig. 9. displays the impact of Reynolds numbers on the average Nusselt and Sherwood numbers on the left wall when Le = 1 for different Richardson and Darcy numbers parameters. The average Sherwood and Nusselt numbers rise due to rising Reynolds numbers. Due to the dominance of thermal diffusion, the most significant Nusselt number and the highest value of the Sherwood number occur at high Richardson numbers due to thermal instabilities and forced flow. Rising Richardson numbers cause the buoyant force to increase as they get closer to natural convection, which affects the heat transfer process and raises the average Nusselt number. When Da increases, more fluid flows can be thrown in the geometry due to high permeability, which means more heat is removed from the system. From the figure, it is clear that both Sh_{avg} and Nu_{avg} decrease by increasing Da. The same behavior can be seen in Case 2, as shown in Fig. 10 to Fig. 14.

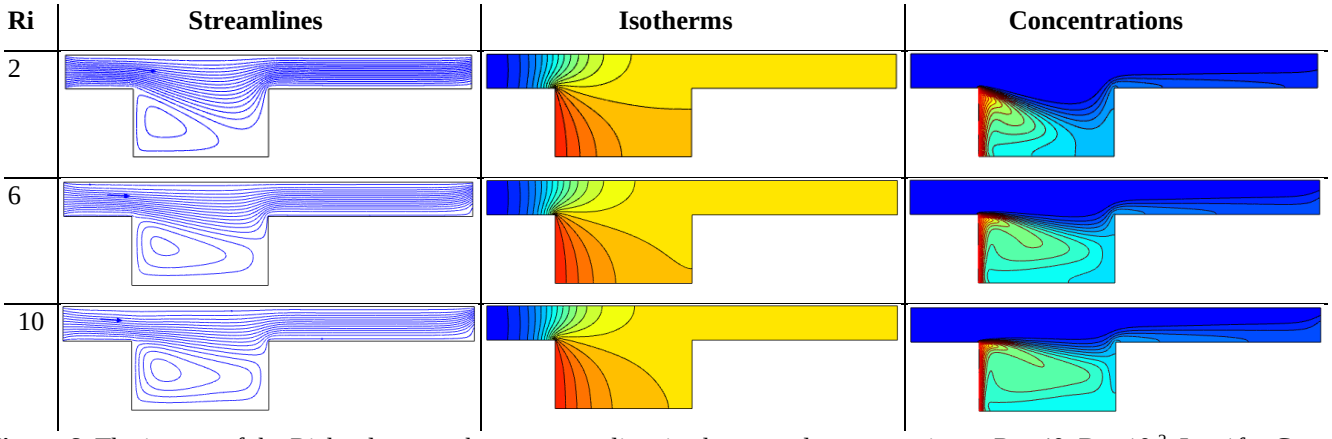

Figure 6. The impact of the Richardson number on streamline, isotherm, and concentration at Re=40, Da=10^{-2}, Le=1for Case 1

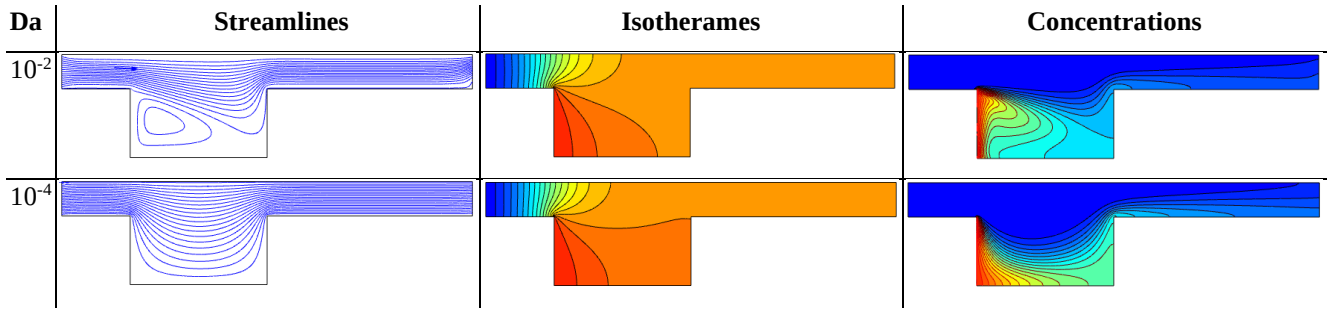

Figure 7. The impact of the Darcy number on streamlines, isotherms, and concentrations at Re=20, Ri=6, Le=1 for Case 1

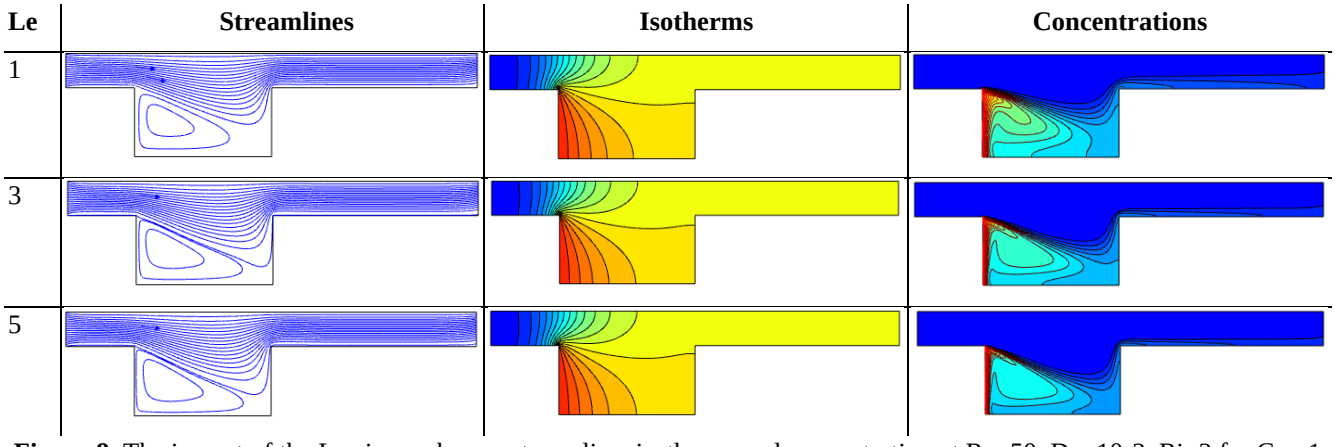

Figure 8. The impact of the Lewis number on streamline, isotherm, and concentration at Re=50, Da=10-2, Ri=2 for Case1

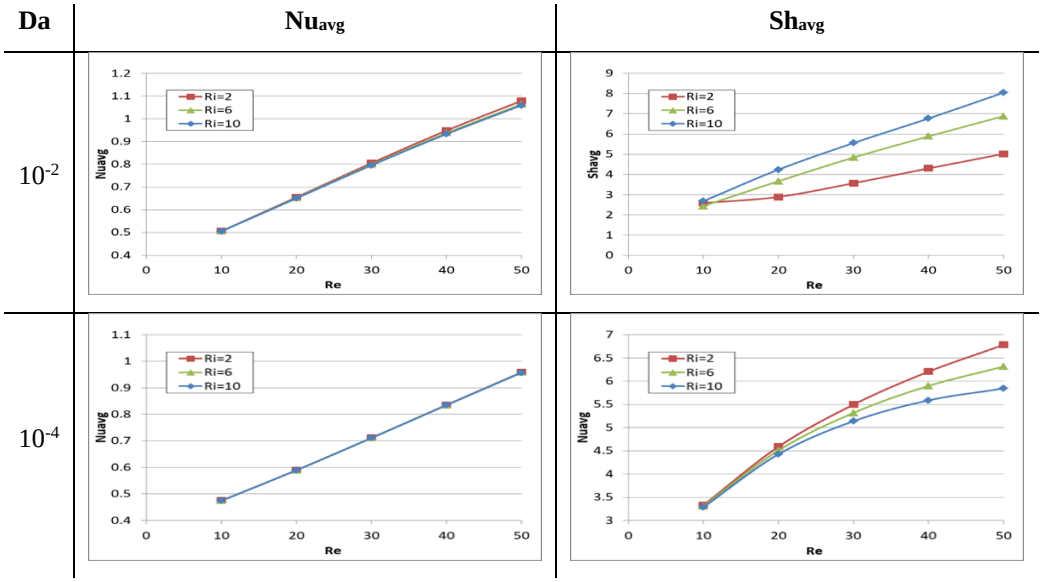

Figure 9. Averaging the Sherwood and Nusselt numbers for different Reynolds, Richardson, and Darcy numbers at Le=1 for Case 1

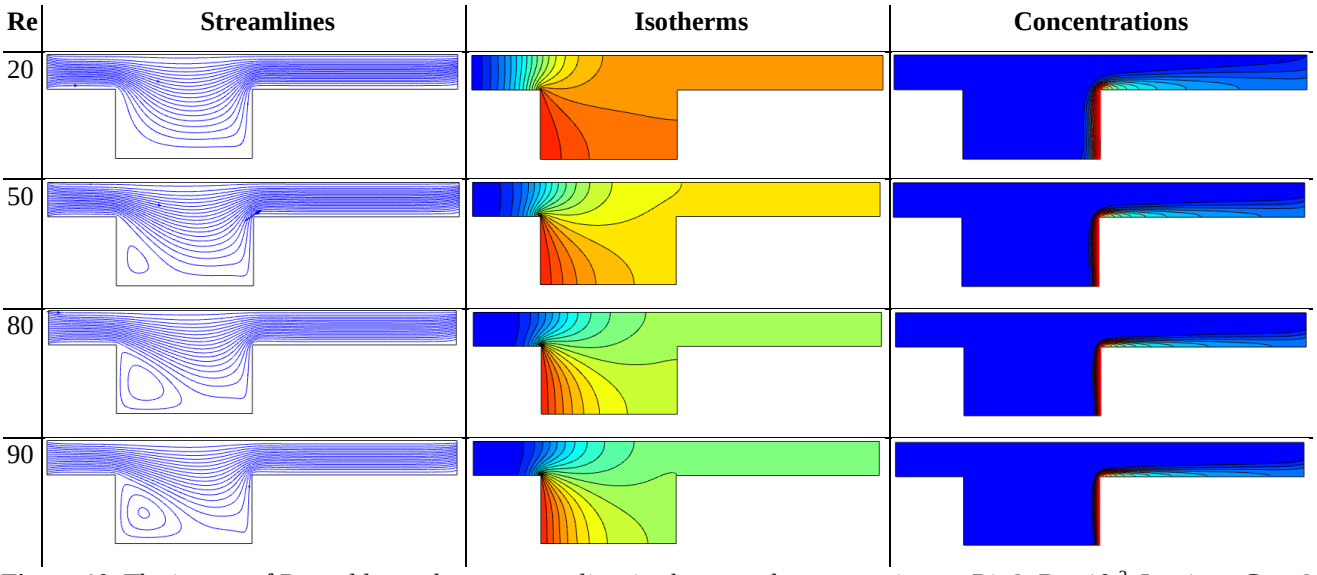

Figure 10. The impact of Reynolds number on streamline, isotherm, and concentrations at Ri=2, Da=10^{-2}, Le=1 sor Case 2

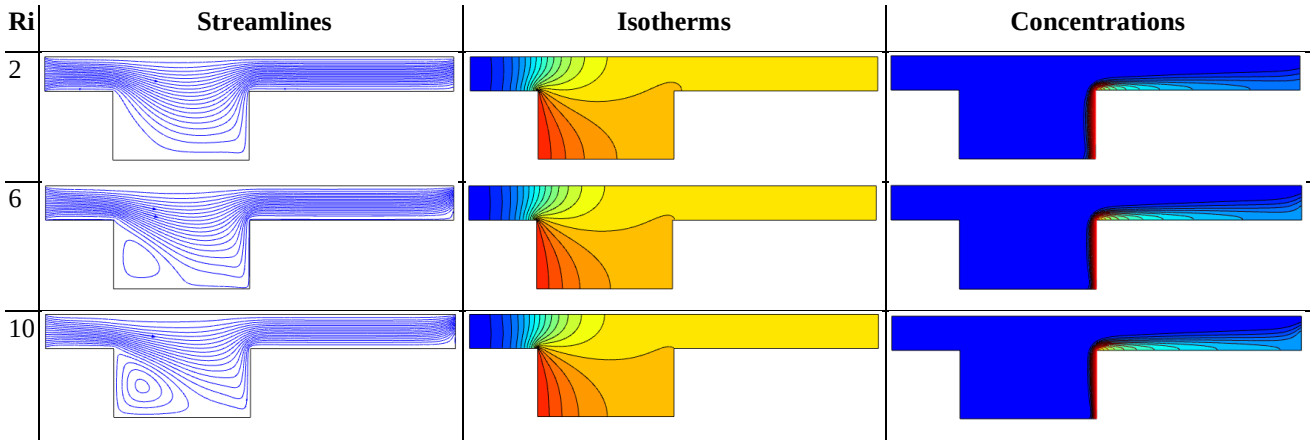

Figure 11. The impact of the Richardson number on streamline, isotherm, and concentration at Re=40, Da=10^{-2}, Le=1 for Case 2

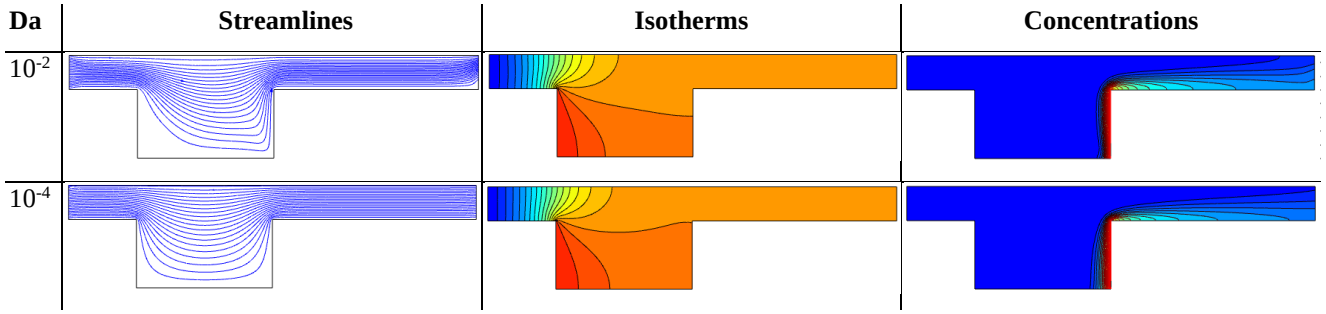

Figure 12. The impact of the Darcy number on streamlines, isotherms, and concentrations at Re=20, Ri=6, Le=1 for Case 2

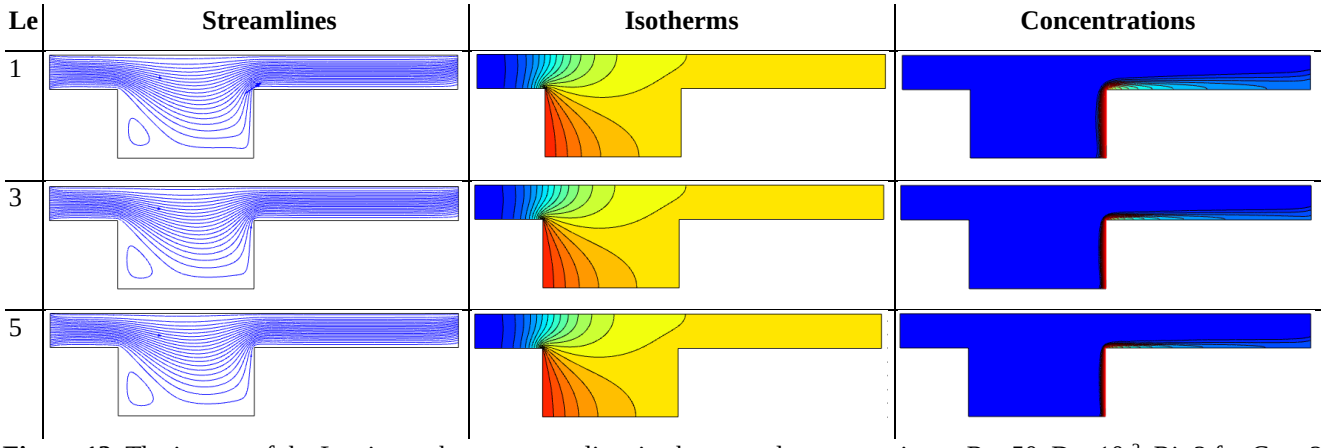

Figure 13. The impact of the Lewis number on streamline, isotherm, and concentration at Re=50, Da=10^{-2}, Ri=2 for Case 2

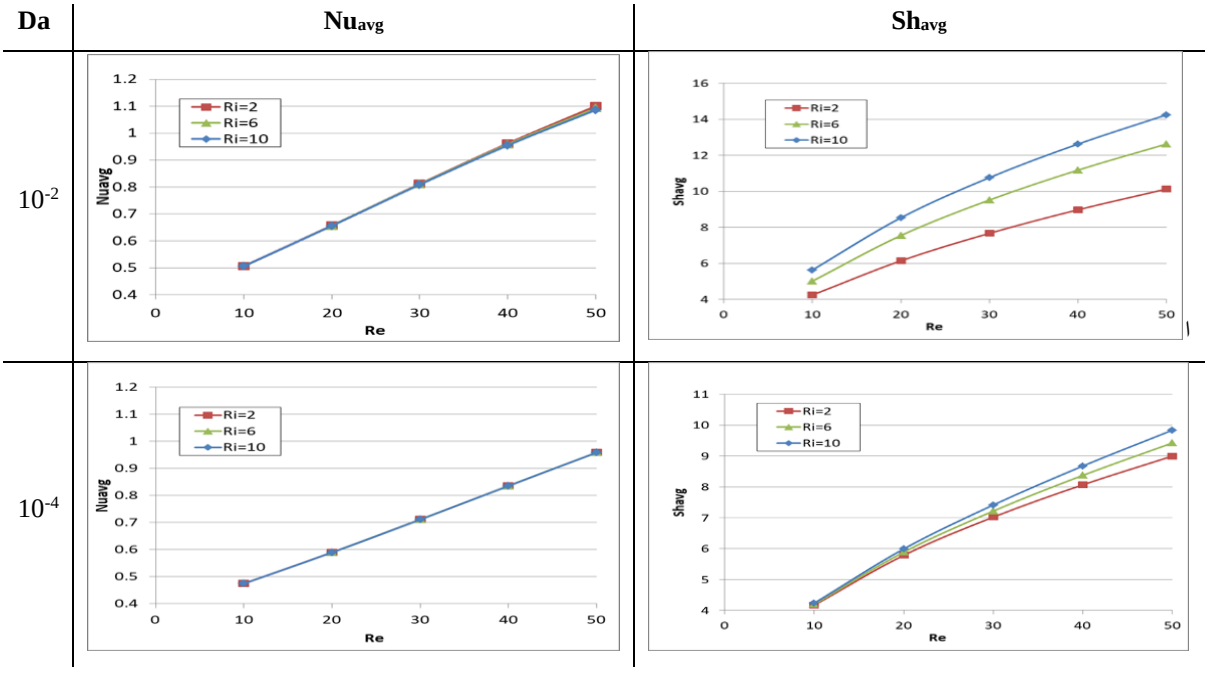

Figure 14. Averaging the Sherwood and Nusselt numbers for different Reynolds, Richardson, and Darcy numbers for Case2

5. Conclusions

This work focuses on numerically investigating the double-diffusive mixed convection flow in a channel with a Cu-Al_2O_3 hybrid nanofluid in a porous media. In this work, the concentration location has been examined in two different scenarios. with a wide range of variables, including ; ($10 \leq Re \leq 100$),($2 \leq Ri \leq 10$), ($Da=10^{-2},10^{-4}$), Lewis number ($1 \leq Le \leq 5$), N = 1, ϕ=0.02, and Pr = 6.2.

It is possible to summarise the impact of physical characteristics on fluid flow movement and the heat and mass transfer as follows.:

- When the Reynolds number is raised to 100, heat and mass transfer significantly increase; the simulation findings show that increased recirculation results from a higher Richardson number.
- In the opposite scenario, mass transfer and heat are both higher.
- Increasing the Richardson number enhances the process of heat transfer.

For a high Darcy number ($Da = 10^{-2}$), there is an increase in heat and mass transfer. Future work will focus on studying heat and mass transfer by mixed convection in a different-shaped channel filled with hybrid nanofluids with/without a porous medium. To complement the current investigations, two- or multiphase flow with or without a porous medium could be incorporated. Future research can investigate mixed convection and entropy generation for hybrid nanofluids within porous cavities with and without Soret and Dufour effects.

List of symbols

CFD Computational Fluid Dynamics
g gravitational acceleration
Gr Grashof number
Kr thermal conductivity ratio, Kr=Kp/Kf
L length of the cavity
Nu local Nusselt number
Nu_{avg} average Nusselt number
P non-dimensional pressure
p pressure
Pr Prandtl number
Re Reynolds number
Ri Richardson number
Sh Sherwood number
Sh_{avg} average Sherwood number
T dimensional temperature
U, V dimensionless velocity components
u,v velocity components in the x- and y-direction
X, Y dimensionless coordinates
x,y horizontal and vertical coordinates

Greek symbols

A thermal diffusivity
β thermal expansion coefficient
ε porosity of the porous medium
θ dimensionless temperature
μ dynamic viscosity
ν kinematic viscosity
ρ density
Ψ streamlines

Subscripts

c cold temperature
f fluid
h hot temperature
p plastic

Acknowledgments

The authors would like to thank the University of Al-Qadisiyah for supporting this research work.

Conflict of interest

The authors declare that there are no conflicts of interest regarding the publication of this manuscript.

Author Contribution Statement

Karrar Kadhim Jaber: Proposed the research problem, coding, ran the simulation, and validation.

Khaled Al-Farhany: Coding, analyzing, writing, and discuss the results, and supervising.

Dhafer A. Hamzah: Confirmed validity and efficacy, methodology, and supervision.

Wael Al-Kouz: discussed the results and contributed to the final manuscript.

References

[1] A. Abdulkadhim, K. Al-Farhany, A. M. Abed, and H. Sh. Majdi, "Comprehensive Review of Natural Convection Heat Transfer in Annulus Complex Enclosures," *Al-Qadisiyah Journal for Engineering Sciences*, vol. 13, no. 2, pp. 80-90, 2020, doi: https://doi.org/10.30772/qjes.v13i2.633.

[2] M. A. Alomari *et al.*, "Magnetohydrodynamic mixed convection in lid-driven curvilinear enclosure with nanofluid and partial porous layer," *Journal of Magnetism and Magnetic Materials*, Article vol. 582, 2023, Art no. 170952, doi: https://doi.org/10.1016/j.jmmm.2023.170952.

[3] M. A. Ghurban, K. Al-Farhany, and K. Benhanifia, "Effects of fin on mixed convection heat transfer in a vented square cavity: A numerical study," *Al-Qadisiyah Journal for Engineering Sciences*, Article vol. 16, no. 3, pp. 200-208, 2023, doi: https://doi.org/10.30772/qjes.2023.142305.1016.

[4] F. Zafar and M. M. Alam, "Mixed convection heat transfer from a circular cylinder submerged in wake," *International Journal of Mechanical Sciences*, vol. 183, p. 105733, 2020/10/01/ 2020, doi: https://doi.org/10.1016/j.ijmecsci.2020.105733.

[5] W. A. Sabbar, M. A. Ismael, and M. Almudhaffar, "Fluid-structure interaction of mixed convection in a cavity-channel assembly of flexible wall," *International Journal of Mechanical Sciences*, vol. 149, pp. 73-83, 2018, doi: https://doi.org/10.1016/j.ijmecsci.2018.09.041.

[6] E. M. Elsaid and M. S. Abdel-Wahed, "Mixed convection hybrid-nanofluid in a vertical channel under the effect of thermal radiative flux," *Case Studies in Thermal Engineering*, vol. 25, p. 100913, 2021, doi: https://doi.org/10.1016/j.csite.2021.100913.

[7] L. Jahanshaloo, E. P. Kermani, and N. A. Che Sidik, "Numerical Prediction of Nanofluid Flow in Channel with Heated Cavity," *Journal of Computational and Theoretical Nanoscience*, vol. 12, no. 9, pp. 2442-2447, 2015, doi: https://doi.org/10.1166/jctn.2015.4045.

[8] B. Ruhani, D. Toghraie, M. Hekmatifar, and M. Hadian, "Statistical investigation for developing a new model for rheological behavior of

ZnO–Ag (50%–50%)/Water hybrid Newtonian nanofluid using experimental data," *Physica A: Statistical Mechanics and its Applications*, vol. 525, pp. 741-751, 2019, doi https://doi.org/10.1016/j.physa.2019.03.118.

[9] A. Raisi, S. Aminossadati, and B. Ghasemi, "Magnetohydrodynamic mixed convection of a cu-water nanofluid in a vertical channel," *Journal of heat transfer*, vol. 135, no. 7, p. 074501, 2013, doi: https://doi.org/10.1115/1.4023880.

[10] E. Manay, E. Mandev, and R. O. Temiz, "Analysis of mixed convection heat transfer of nanofluids in a minichannel for aiding and opposing flow conditions," *Heat and Mass Transfer*, vol. 55, no. 10, pp. 3003-3015, 2019, doi: https://doi.org/10.1007/s00231-019-02638-6.

[11] S. Sindhu, B. Gireesha, and D. Ganji, "Simulation of Cu: γ–ALOOH/Water in a microchannel heat sink by dint of porous media approach," *Case Studies in Thermal Engineering*, vol. 21, p. 100723, 2020, doi: https://doi.org/10.1016/j.csite.2020.100723.

[12] K. Al-Farhany, M. A. Alomari, A. Al-Saadi, A. Chamkha, H. F. Öztop, and W. Al-Kouz, "MHD mixed convection of a Cu–water nanofluid flow through a channel with an open trapezoidal cavity and an elliptical obstacle," *Heat Transfer*, vol. 51, no. 2, pp. 1691-1710, 2022, doi https://doi.org/10.1002/htj.22370.

[13] M. A. Qureshi, S. Hussain, and M. A. Sadiq, "Numerical simulations of MHD mixed convection of hybrid nanofluid flow in a horizontal channel with cavity: Impact on heat transfer and hydrodynamic forces," *Case Studies in Thermal Engineering*, vol. 27, p. 101321, 2021, doi: https://doi.org/10.1016/j.csite.2021.101321.

[14] F. J. Gumir, K. Al-Farhany, W. Jamshed, E. S. M. Tag El Din, and A. Abd-Elmonem, "Natural convection in a porous cavity filled (35% MWCNT-65% Fe3O4)/water hybrid nanofluid with a solid wavy wall via Galerkin finite-element process," *Scientific Reports*, vol. 12, no. 1, p. 17794, 2022, doi: https://doi.org/10.1038/s41598-022-22782-0.

[15] K. Al-Farhany, M. A. Alomari, and A. E. Faisal, "Magnetohydrodynamics Mixed Convection Effects on the open enclosure in a horizontal channel Heated Partially from the Bottom," in *IOP Conference Series: Materials Science and Engineering*, 2020, vol. 870, no. 1: IOP Publishing, p. 012174, doi: https://doi.org/10.1088/1757-899x/870/1/012174.

[16] K. Al-Farhany, M. A. Alomari, A. Albattat, and A. J. Chamkha, "MHD mixed convection on Cu-water laminar flow through a horizontal channel attached to two open porous enclosure," *The European Physical Journal Special Topics*, vol. 231, no. 13, pp. 2851-2864, 2022, doi: https://doi.org/10.1140/epjs/s11734-022-00589-4.

[17] B. Buonomo, O. Manca, L. Marinelli, and S. Nardini, "Mixed convection in horizontal channels heated below with external heat losses on upper plate and partially filled with aluminum foam," 2014. [Online]. Available: https://dc.engconfintl.org/porous_media_V/14/.

[18] A. Barletta and D. Rees, "Unstable mixed convection flow in a horizontal porous channel with uniform wall heat flux," *Transport in Porous Media*, vol. 129, pp. 385-402, 2019, doi: https://doi.org/10.1007/s11242-019-01294-y.

[19] R. Nath and M. Krishnan, "Numerical study of double diffusive mixed convection in a backward facing step channel filled with Cu-water nanofluid," *International Journal of mechanical Sciences*, vol. 153, pp. 48-63, 2019, doi: https://doi.org/10.1016/j.ijmecsci.2019.01.035.

[20] A. Q. Abd Al-Hassan and M. A. Ismael, "Numerical study of double diffusive mixed convection in horizontal channel with composite open porous cavity," *Special Topics & Reviews in Porous Media: An International Journal*, vol. 10, no. 4, 2019, doi: https://doi.org/10.1615/specialtopicsrevporousmedia.2019029342.

[21] K. Al-Farhany and A. Turan, "Numerical study of double diffusive natural convective heat and mass transfer in an inclined rectangular cavity filled with porous medium," *International Communications in Heat and Mass Transfer*, vol. 39, no. 2, pp. 174-181, 2012, doi: https://doi.org/10.1016/j.icheatmasstransfer.2011.11.014.

[22] K. Al-Farhany and A. Turan, "Double-Diffusive of Natural Convection in an Inclined Porous Square Domain Generalized Model," *Al-Qadisiyah Journal for Engineering Sciences*, vol. 12, no. 3, pp. 151-160, 2019, doi: https://doi.org/10.30772/qjes.v12i3.612.

[23] S. Aminossadati and B. Ghasemi, "Natural convection cooling of a localised heat source at the bottom of a nanofluid-filled enclosure," *European Journal of Mechanics-B/Fluids*, vol. 28, no. 5, pp. 630-640, 2009, doi: https://doi.org/10.1016/j.euromechflu.2009.05.006.

[24] H. T. Kadhim, F. A. Jabbar, and A. Rona, "Cu-Al2O3 hybrid nanofluid natural convection in an inclined enclosure with wavy walls partially layered by porous medium," *International Journal of Mechanical Sciences*, vol. 186, p. 105889, 2020, doi: https://doi.org/10.1016/j.ijmecsci.2020.105889.

[25] S. Hussain, K. Mehmood, M. Sagheer, and A. Farooq, "Entropy generation analysis of mixed convective flow in an inclined channel with cavity with Al2O3-water nanofluid in porous medium," *International Communications in Heat and Mass Transfer*, vol. 89, pp. 198-210, 2017, doi: https://doi.org/10.1016/j.icheatmasstransfer.2017.10.009.

[26] K. Al-Farhany, M. A. Alomari, N. Biswas, A. Laouer, A. M. Abed, and W. Sridhar, "Magnetohydrodynamic double-diffusive mixed convection in a curvilinear cavity filled with nanofluid and containing conducting fins," *International Communications in Heat and Mass Transfer*, vol. 144, p. 106802, 2023/05/01/ 2023, doi: https://doi.org/10.1016/j.icheatmasstransfer.2023.106802.